Turkish J. Eng. Env. Sci.
31 (2007) , 149 – 156.


# Production and Characterization of High Porosity Ti-6Al-4V Foam by Space Holder Technique in Powder Metallurgy

**Güher KOTAN, A. Şakir BOR**
*Middle East Technical University, Metallurgical and Materials Engineering, Ankara, 06531, TURKEY*
*e-mail: guher@metu.edu.tr*

Received 25.08.2006

**Abstract**

The present study was undertaken to investigate the production of a high porosity, biocompatible Ti-6Al-4V alloy by space holder technique using spherical carbamide particles, and to characterize the produced samples by compression tests and SEM images. The technique includes the following steps: mixing of 100-600 $\mu$m diameter spherical carbamide particles with irregular Ti-6Al-4V alloy powder of $<$78 $\mu$m size, compaction of the mixture of carbamide particles and Ti-6Al-4V powders by cold uniaxial die pressing, removal of carbamide by melting and dissociation, and sintering of the compact. Optimum compaction pressure, which preserves carbamide sphericity while providing the required packing of Ti alloy powders, was found to be 450 MPa. Ti-6Al-4V alloy foams of porosities between 60% and 75% with mean pore sizes of $\sim$400 $\mu$m and mean sphericity values of 0.65 were successfully produced. Yield strength was observed to exponentially decrease with porosity, which is typical of cellular metals, reaching significantly low values at around 65% porosity, which was thought to be a result of pore coalescence.

**Key words:** Foam, Carbamide, Porosity, Ti6Al4V alloy, Space holder, Compression testing.

## Introduction

In the development of materials science, mimicking nature led to the production of materials like foams, composites, and synthetic polymers as indicated by Gibson and Ashby (1988). This point of view has led to an increase in the studies on production of foams and hence porous metals. These exceptionally lightweight materials possess unique combination of properties, such as impact energy absorption capacity, air and water permeability, unusual acoustic properties, low thermal conductivity, good electrical insulating properties, and high stiffness due to very low specific weight as stated by Banhart (2001).

Biomaterial science has succeeded in producing biocompatible implants that mimic nature. One of the important developments in this field is the usage of titanium and its alloys as structural implants due to their high corrosion resistance, good mechanical properties, and unique biocompatibility among all other metals as indicated by Rao et al. (1997).

As Wen et al. (2001) have revealed, titanium and titanium alloy foams are not only biocompatible but also their open-cellular structure with a mean pore size of 200-500 $\mu$m permits the ingrowth of the new bone tissue and the transport of body fluids. Moreover, the mechanical properties of cellular structures can be adjusted by modifying the amount, morphology, and size of the pores. This is a key characteristic of Ti-6Al-4V foam structures in bone implant applications because it gives the opportunity to obtain mechanical properties compatible with the bone and so prevents the stress-shielding problem that exists in the implantation of bulk materials due to the mismatch of elastic modulus and strength.

As stated by Banhart (2001), there are numerous methods of foam production. Early attempts concentrated on foaming techniques with gas serving as the foaming agent, followed by the development

of new production methods as a result of increasing demand for different structures and properties, such as high porosity and interconnection between pores. Some of the casting methods employed to produce highly porous and interconnected cellular structure are as follows: casting liquid metal around loosely packed inorganic/organic granules or hollow spheres, introducing such space holder materials into a metallic melt prior to casting, and casting a molten metal directly into a polymeric porous material. After casting, the granules or the polymeric porous media can be removed by leaching in suitable solvents or acids or by thermal treatment as indicated by Banhart (2001). One further possibility is to melt powder compacts containing a gas-releasing foaming agent.

Metallic foams can also be produced by metallic deposition on reticulated urethane substrates. Some powder metallurgy techniques including slurry foaming, loose powder sintering, and fiber metallurgy have also been used for the production of high porosity metals as indicated by Banhart (2001). In the case of titanium, due to its high activity at molten state, most of the above-mentioned production methods are not preferred or the methods can give limited porosity as in the case of loose powder sintering. In this stage, the powder metallurgy technique using space holder material comes into picture with its advantages like adjustable pore size distribution, pore shape, and porosity amount. Especially in the production of high porosity Ti, the space holder technique using carbamide has succeeded in the studies by Bram et al. (2000), Wen et al. (2001), and Laptev et al. (2004). However, in these studies neither the technique concerning the removal procedure of the foaming agent nor the production parameters was clearly revealed. Therefore, in this study optimization of the parameters of Ti alloy foam production using carbamide as space holder was investigated with emphasis on the morphological features and mechanical properties of the Ti-6Al-4V foam produced.

## Materials Used and Experimental Procedure

Ti-6Al-4V alloy powders of less than 78 $\mu$m size with a nominal size of 58 $\mu$m were used in the experiments. The powders were irregular in shape and conform to ASTM 1580-01 (Figure 1). As a space holder material, carbamide, also named urea, was chosen due to its advantages of shape and ease of removal prior to sintering (Figure 2). Spherical carbamide particles were sieved to the size range of 0.6-1.0 mm.

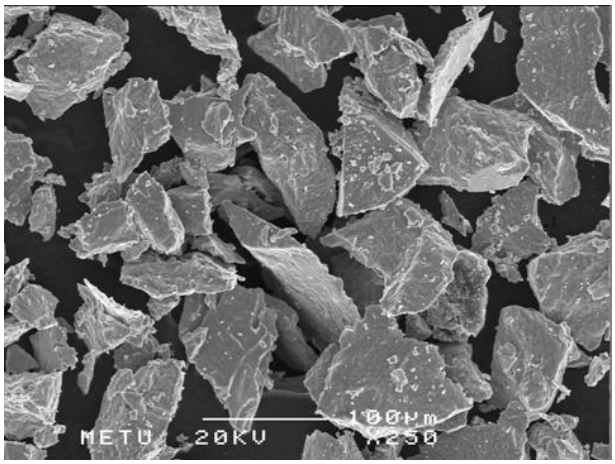


**Figure 1.** Ti-6Al-4V alloy powders of irregular shape.


**Figure 2.** Carbamide particles with a size range of 0.6-1.0 mm.

Initially, 0.6-1.0 mm range carbamide particles were dissolved in water for 10 s to decrease the size to 0.2-0.6 mm preserving sphericity. They were then mixed with Ti-6Al-4V alloy powders manually in a ceramic bowl. The mixture containing carbamide particles and Ti-6Al-4V alloy powders was weighed and placed into a cylindrical steel mold of 15 mm diameter for compaction by conventional cold uniaxial press with compaction pressures in the range from 100 to 450 MPa. The samples were heated up to ~193 °C from room temperature in 4 h in a vertical furnace through which upward flow of high purity argon gas was maintained during the removal of carbamide and sintering in order to ease the removal of gaseous carbamide and its dissociation products

while avoiding the oxidation of Ti alloy. Dissociation was carried out at ∼193 °C for 6-10 h depending on the size of the sample. Then the sample was heated up to 450 °C in 30 min to remove the remnant carbamide.

After the complete removal of carbamide and its dissociation products sintering was conducted at ∼1080 °C for ∼2 h under protective argon atmosphere. At the end of sintering, the samples were drawn to the cold zone of the furnace and cooled to room temperature at a rate close to air cooling before the furnace seal was broken. Densities of the produced specimens were determined geometrically from the measured weight and dimensions. The shape of the specimens was very critical in these measurements, and at very high porosities, due to shape distortion, the density measurements were not very accurate. Therefore, in this study, samples with porosities higher than 75% were not characterized due to shape distortion.

Mechanical characterization of the samples was carried out by compression tests performed on a Shimadzu tension-compression testing machine. After grinding both the top and bottom surfaces of the sample, grease was applied to reduce the friction between the sample and the die surfaces. Samples with h/d ratios of 0.6-1 were compressed at a cross head speed of 0.5 mm/min. For the determination of the yield strength 0.002 the offset method was used.

Scanning electron microscope (SEM) images of the samples obtained by JSM 6400 were used to determine the pore size and pore shape distributions by a commercial image analyzer program, Clemex. For microstructural investigation, the porous samples were first molded into a resin to fill the pores, so that the pore walls were prevented from destruction during grinding and polishing. The samples were etched by 6 ml of $HNO_3$+ 3 ml of HF + 100 ml of deionized water subsequent to emery paper grinding and polishing with 10 $\mu$m and 1 $\mu$m alumina in succession. SEM images made it possible to observe the details of pore morphology, microstructure, pore walls, and sintering behavior.

## Results and Discussion

It must be noted that, in the production, compaction pressure, carbamide removal procedure and selected temperatures were all outcomes of studies held with numerous samples and as a result the optimum procedure as explained in the experimental technique was developed.

Concerning the compaction stage, it has been found that at pressures below 300 MPa samples cannot remain intact after the removal of the carbamide. In view of this fact, optimum compaction pressure leading to a sound product is determined as 450 MPa for Ti-6Al-4V alloy powders mixed with carbamide.

Ti-6Al-4V alloys with porosities ranging between 60% and 75% were successfully produced. Figure 3, obtained using the image analyzer program Clemex, shows pore size distribution in terms of spherical diameter of a 64% porous alloy with expected pore size of less than 700 $\mu$m. The observed pores of sizes above 700 $\mu$m indicate the amount of pore coalescence, which corresponds to ∼4% of the total pores. Figure 4 presents the SEM image of a 64% porous sample where pore coalescence can clearly be observed.

Pore morphology is also investigated by image analyzer in terms of sphericity value, defined as the a/b ratio of the presumed ellipsoidal shape, where a and b are the minor and major axes, respectively. Figure 5 shows the sphericity distribution of the pores for 61% porous sample; it can be seen that sphericity values of pores are above 0.5 for 80% of the pores with an average of 0.65, which can be interpreted as a sufficiently high sphericity.

A closer view of pore walls can be observed in Figures 6 and 7. The interconnected, angular-shaped micro pores apparent at the pore walls suggest that sintering is only at the initial stage. This can be understood not only from the non-spherical interconnected morphology of the micro pores but also from the relative neck size to powder size ratio, which is obviously lower than 0.3 and representative of the initial stage of sintering as elucidated by German (1994). During sintering at ∼1080 °C for ∼2 h, compacted Ti-6Al-4V powders at the pore walls have completed the rearrangement and have started neck formation but, because of insufficient diffusivity, neck growth and hence the sintering has not been completed. Partial sintering and presence of micro pores are not expected to affect the pore characteristics to any significant extent except causing a slightly larger pore size due to geometrical reasons, but the micro pores obviously deteriorate the mechanical properties by reducing the load bearing cross-sectional area of the pore walls.

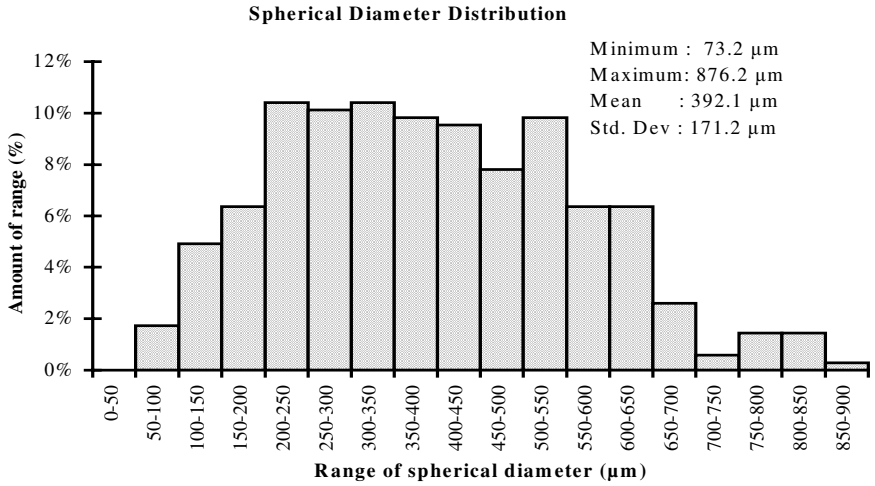


**Figure 3.** Spherical diameter (pore size) distribution of 64% porous Ti-6Al-4V foam.

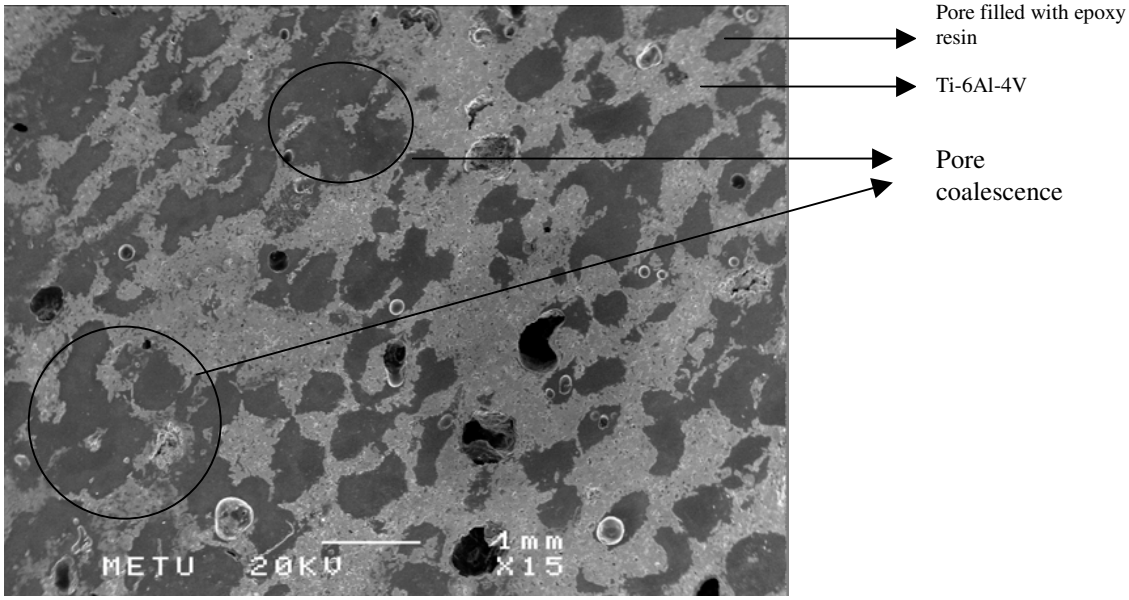


**Figure 4.** SEM image of 64% porous Ti-6Al-4V foam.

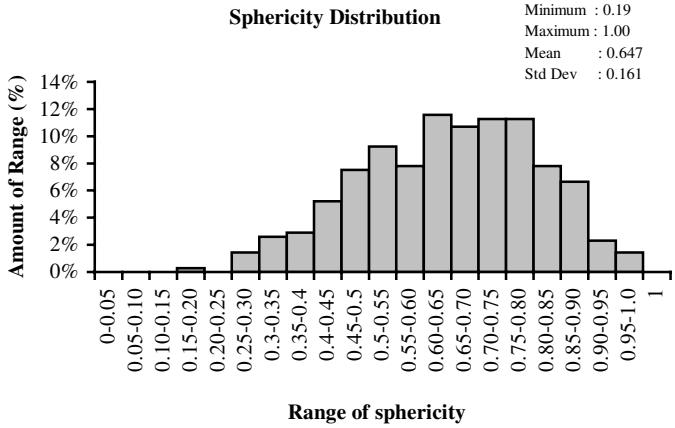


**Figure 5.** Sphericity distribution of 61% porous Ti-6Al-4V foam.

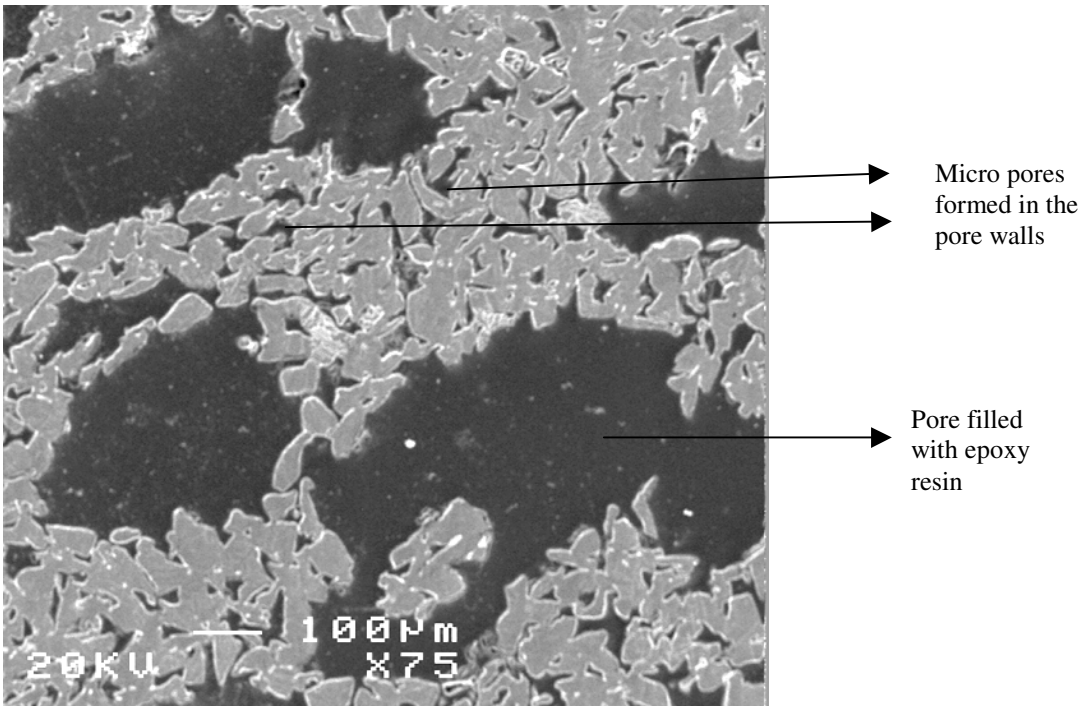


**Figure 6.** SEM image of a closer view of the pore walls.

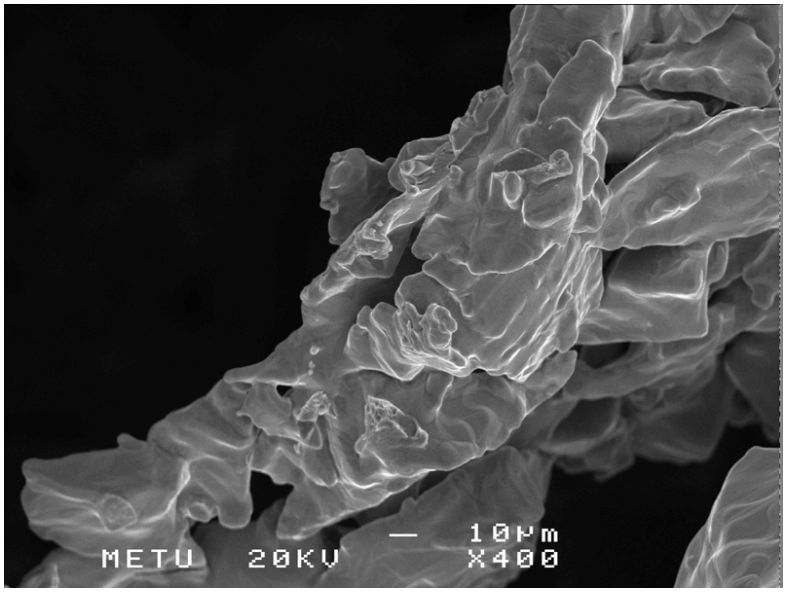


**Figure 7.** SEM image of sintered Ti-6Al-4V powders at the pore walls, showing incomplete sintering since most of the powder particles can be easily distinguished from each other.

Microstructure of the etched sample cooled relatively slowly from the sintering temperature, which corresponds to a single beta phase region, to room temperature where the equilibrium phases are alpha (hcp) and beta (bcc) can be seen in Figure 8. Alpha phase with higher vanadium solubility can be observed as the matrix, while the beta phase with lower vanadium solubility appears as platelets displaying the morphology also known as Widmanstätten structure.

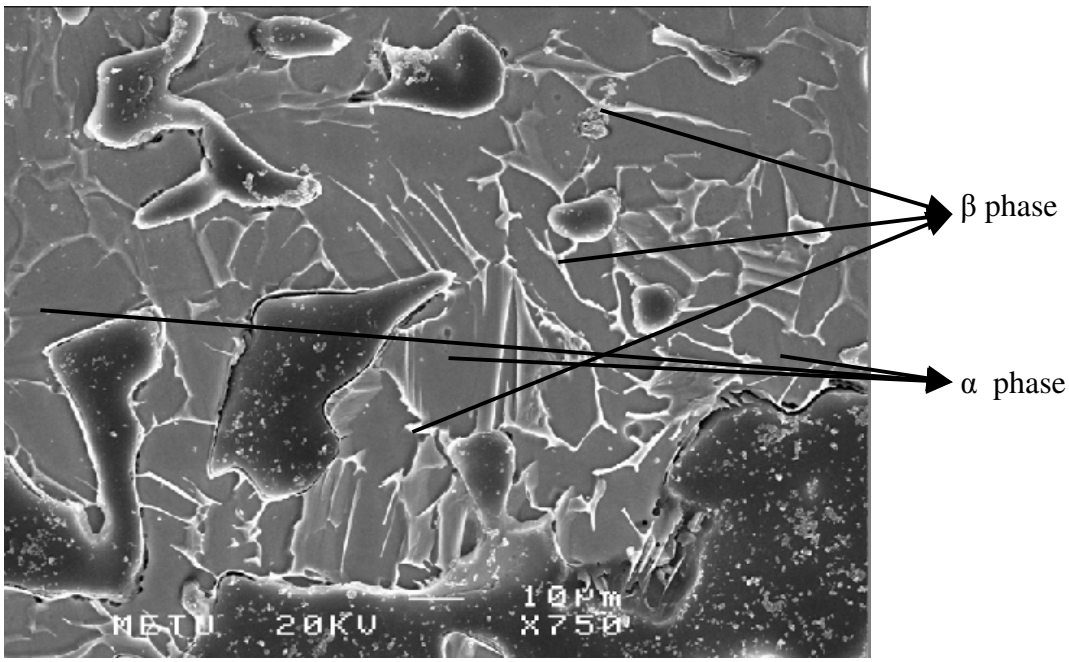


**Figure 8.** Microstructure of Ti-6Al-4V obtained after furnace cooling.

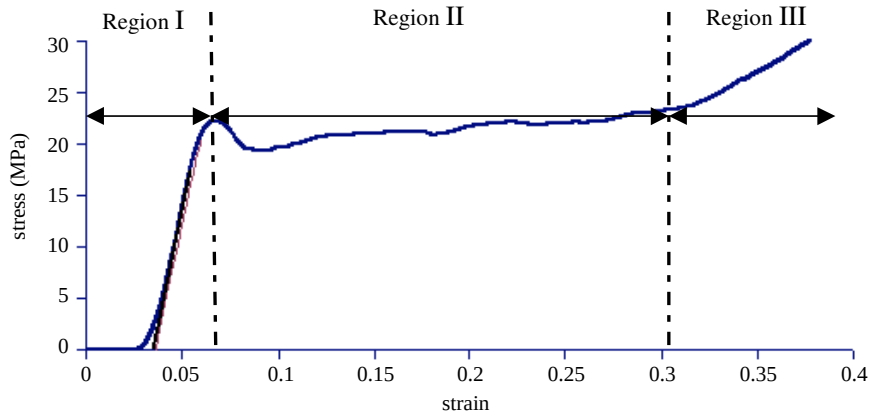


**Figure 9.** A typical compression test result for 75% porous Ti foam.

The compressive behavior of cellular metals is very interesting due to their high energy absorption capacity. Typical compression test behavior of titanium foam of 75% porosity is given in Figure 9. The graph is divided into 3 main parts: the initial part is the elastic region where yielding is observed; then it is followed by a plateau region through which the pores are compressed and distorted. At this region the energy absorption can be observed because until a certain amount of pore collapse the stress level is maintained at a constant value. At the end of the plateau stress starts to increase because since the pores at the deformation zone have flattened the material behavior shifts to a bulk material behavior under compression.

Figures 10 and 11 show the change in compressive yield strength and elastic modulus of the foam, respectively, with porosity, where both decrease with increasing porosity. The important point in this behavior is that the relation between strength-porosity and elastic modulus-porosity is exponential as predicted by the Gibson-Ashby model for cellular solids, which states that the relationship is non-linear. The strength values determined in this study are lower than those predicted by the theoretical models because the models assume bulk values for the pore

walls. However, since only the initial stage of sintering is performed there are large numbers of micro pores formed in the walls and therefore they cannot be considered bulk material. At the initial stage of sintering although neck formation has started, since the neck area is very small, stress on the neck area is much higher than it would be for a solid pore wall. Furthermore, the interconnection of micro pores eases the crack propagation along the already existing surfaces. Therefore, an incomplete sintering process resulted in lower wall strength yielding a lower overall strength.

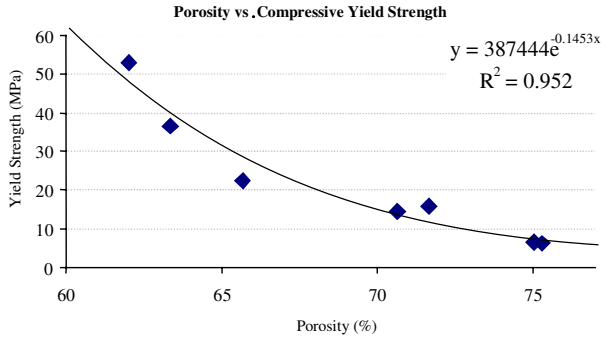


**Figure 10.** Compressive yield strength changes with porosity.

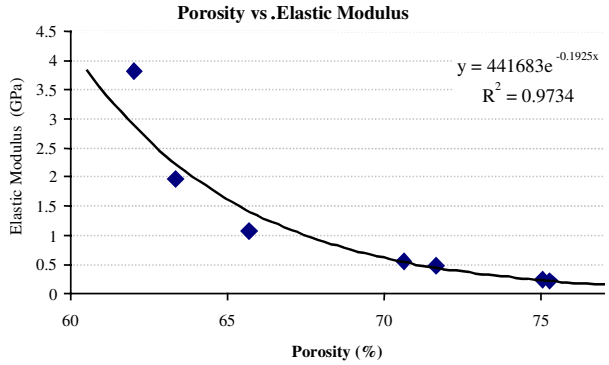


**Figure 11.** Elastic modulus changes with porosity.

It is noteworthy that the change in the yield strength is significant at around 65%, which can be related to an increase in pore coalescence with increasing porosity.

## Conclusion

Our study resulted in the successful production of Ti-6Al-4V foam in the 60%-75% porosity range with mean pore sizes of $\sim$ 400 $\mu$m and sphericity value of $\sim$0.65, using carbamide as space holder. The mechanical behavior of open cellular foams was observed via compression tests and a non-linear relationship (probably exponential) was detected between mechanical properties and porosity. The mechanical properties were found to be much lower than expected from idealized models and the target theoretical values were attributed to the inefficient sintering resulting in interconnected micro pores in the load bearing pore walls. Hence, a sintering temperature of 1080 °C was found to be insufficient for sintering Ti-6Al-4V foams by this technique to achieve the desired mechanical properties.

It was also observed that mechanical properties degrade significantly above 65% porosity due to changes in the pore structure, i.e. pore coalescence.

## Acknowledgment

We would like to thank TÜBİTAK for funding our project (104M121).

## References

Banhart, J., "Manufacture, Characterisation and Application of Cellular Metals and Metal Foams", Progress in Materials Science, 46, 6, 559-632, 2001.

Bram, M., Stiller, C., Buchkremer, H.P., Stöver, D. and Bauer, H.; "High-Porosity Titanium, Stainless Steel, and Superalloy Parts", Advanced Engineering Materials, 2, 196-199, 2000.

Gibson, L.J. and Ashby, M.F., Cellular Solids; Structure and Properties, Second Edition, Cambridge University Press, Cambridge, 1988.

German, R.M., Powder Metallurgy Science, Metal Powder Industries Federation, Princeton, New Jersey, 1994.

Laptev, A., Bram, M., Buchkremer H.P. and Stöver D., "Study of Production Route for Titanium Parts Combining Very High Porosity and Complex Shape", Powder Metallurgy, 47, 85-92, 2004.

Rao, S., Okazaki, Y. and Tateishi, T., "Cytocom-

patibility of New Ti Alloy Without Al and V by Evaluating the Relative Growth Ratios of Fibroblasts L929 and Osteoblasts MC3T3-E1 cells" , Materials Science and Engineering: C, 4, 4, 311-314, 1997.

Wen, C. E., Mabuchi, M., Yamada, Y., Shimojima, K., Chino, Y. and Asahina, T., "Processing of Biocompatible Porous Ti and Mg", Scripta Materialia, 45, 1147-1153, 2001.